

Inversely Learning Transferable Rewards via Abstracted States

Yikang Gui
University of Georgia
United States
yikang.gui@uga.edu

Prashant Doshi
University of Georgia
United States
pdoshi@uga.edu

ABSTRACT

Inverse reinforcement learning (IRL) has progressed significantly toward accurately learning the underlying rewards in both discrete and continuous domains from behavior data. The next advance is to learn *intrinsic* preferences in ways that produce useful behavior in settings or tasks which are different but aligned with the observed ones. In the context of robotic applications, this helps integrate robots into processing lines involving new tasks (with shared intrinsic preferences) without programming from scratch. We introduce a method to inversely learn an abstract reward function from behavior trajectories in two or more differing instances of a domain. The abstract reward function is then used to learn task behavior in another separate instance of the domain. This step offers evidence of its transferability and validates its correctness. We evaluate the method on trajectories in tasks from multiple domains in OpenAI’s Gym testbed and AssistiveGym and show that the learned abstract reward functions can successfully learn task behaviors in instances of the respective domains, which have not been seen previously.

KEYWORDS

Abstraction; Inverse reinforcement learning; Transfer learning

ACM Reference Format:

Yikang Gui and Prashant Doshi. 2025. Inversely Learning Transferable Rewards via Abstracted States. In *Under review as a conference paper at Proc. of the 24th International Conference on Autonomous Agents and Multiagent Systems (AAMAS 2025), Detroit, Michigan, USA, May 19 – 23, 2025*, IFAAMAS, 10 pages.

1 INTRODUCTION

The objective of inverse reinforcement learning (IRL) is one of abductive reasoning: to infer the reward function that best explains the observed trajectories. This is challenging because the available data is often sparse, which admits many potential solutions (some degenerate), and the learned reward functions may not generalize for use in target instances that could be slightly different. Despite these challenges, significant progress has been made in the last decade toward learning the underlying reward functions in both discrete and continuous domains, which are accurate (in yielding the observed behavior) and parsimonious [3]. A key advance in IRL next is to learn reward functions that represent *intrinsic preferences*, which become relevant in aligned task instances not seen previously. This contributes to the transferability of the learned rewards – an important characteristic of a general solution.

Prior work focused on enabling transferable IRL has been limited. Adversarial IRL [7] sought to disentangle the task dynamics, i.e., the transition function, from the learned reward function. The method does not require knowing the task dynamics and aims to obtain reward functions that yield behavior on tasks whose dynamics can be different, but with limited success. Meta IRL [33] samples trajectories from a distribution of aligned tasks and aims to learn a reward function that generalizes to the distribution. While the learned reward function is more general, it requires significant fine-tuning on unseen tasks.

In this paper, we introduce a new method that generalizes IRL to previously unseen tasks but which exhibit commonality with the observed ones in terms of shared core or intrinsic preferences. Abstractions offer a powerful representation for generalization [1]. We introduce the concept of an abstract reward function, whose learning is influenced through abstracted states. Let us take Ant [27] from OpenAI Gymnasium as an example. Consider two Ant environments with different disabled legs as the source environments and an Ant environment with another pair of disabled legs as the target environment. As source environments and the target environment have different disabled legs, the original marginal state distributions of the sources are different from the target’s, making it difficult to transfer a learned reward function. However, if instead of the ant’s legs, we focus on the torso of the ant, the marginal state distribution of the torso remains mostly the same across both the sources and the target environment as well. In this case, if a reward function based on the torso is learned, which is the *abstraction*, the reward function can be transferred across any disabled legs.

Our method utilizes observed behavior data from two or more differing instances of a task domain as input to a variational autoencoder (VAE). A single encoder is coupled with multiple decoders, one for each instance in order to reconstruct the instance trajectories. We show how the common latent variable(s) of this distinct VAE model can be interpreted and shaped as an abstract reward function that governs the input task behaviors. Note that two or more aligned task behaviors are needed to learn the shared intrinsic preferences in performing the tasks.

We evaluate our method labeled T-IRL on multiple benchmark OpenAI Gym domains [27] and AssistiveGym [5]. We utilize trajectories from two differing instances in each domain as input to the VAE and show how the inversely learned abstract reward function can help successfully learn the correct behavior in a third aligned instance of the domain. These results, though on toy domains, strongly indicate that we may learn abstract reward functions via IRL that offer a level of generalizability not presented previously in the literature. However, it comes at the expense of having two or more aligned task instances, which share common intrinsic preferences.

Under review as a conference paper at Proc. of the 24th International Conference on Autonomous Agents and Multiagent Systems (AAMAS 2025), A. El Fallah Seghrouchni, Y. Vorobeychik, S. Das, A. Nowe (eds.), May 19 – 23, 2025, Detroit, Michigan, USA. © 2025 International Foundation for Autonomous Agents and Multiagent Systems (www.ifaamas.org). This work is licenced under the Creative Commons Attribution 4.0 International (CC-BY 4.0) licence.

2 RELATED WORK

Previous adversarial IRL or imitation learning (IL) methods (AIRL[7], f -MAX [11], SMM [19]) utilize the discriminator to guide the generator to recover a policy that matches the expert’s state-action distribution. They learn a non-stationary reward function through an iterative process involving a discriminator network and policy updates. At each iteration, the discriminator provides a reward signal that induces a single policy update step. However, upon convergence, the learned reward function from the discriminator cannot be directly used to train a new policy from scratch, as it is inherently tied to the specific policy optimization trajectory. Consequently, the reward function is discarded after the learning process. In contrast, f -IRL [22] aims to recover a stationary reward function. This reward function possesses the desirable property that if an arbitrary policy is optimized using this reward until convergence, the resulting policy’s behavior will match the demonstrated expert trajectories.

To address the limitations of adversarial methods like GAIL, IQ-Learn [9] presents a novel non-adversarial approach for IL. IQ-Learn directly learns soft Q-functions from expert data, leveraging the benefits of Q-learning from reinforcement learning (RL) without the need for adversarial training. This method simplifies the IL process, providing a stable, data-efficient, and scalable solution. However, since the soft-Q function involves actions, it is hard to generalize to the state-only reward function.

Tanwani and Billard [29] addresses the challenge of learning diverse strategies for complex tasks from multiple expert demonstrations. Traditional IRL methods often focus on a single expert, which limits their ability to generalize across different strategies. This paper introduces a transfer learning approach that incrementally learns various strategies by leveraging shared knowledge between them, thus improving learning efficiency and performance. Although this paper utilizes transfer learning to learn a transferable reward function, the environment remains the same, therefore the dynamics do not change for source and target domains. Their reward function is transferable among all expert policies.

Indirect Imitation Learning (I2L) [8], a state-only imitation learning algorithm designed to handle transition dynamics mismatches between expert and imitator environments. By minimizing the Wasserstein distance between the expert’s and imitator’s state distributions, I2L avoids the need for expert actions and leverages a priority-based trajectory buffer to stabilize learning. Their approach outperforms baseline methods like GAIfO and GAIL, particularly in continuous control tasks with mismatched dynamics, such as varying gravity or friction in MuJoCo environments. I2L demonstrates strong performance in state-only settings, making it a robust alternative for imitation learning when expert actions are unavailable. I2L relies on a trajectory buffer to approximate these distributions.

Cao et al. [4] address the challenge of reward non-identifiability in inverse reinforcement learning (IRL) by using an entropy regularized framework. Their method identifies rewards by observing multiple optimal policies under different discount rates or transition dynamics. While this approach resolves the ambiguity in recovering rewards, it requires access to these distinct optimal policies, making it less suitable for scenarios where such information is unavailable.

Furthermore, their algorithm is not designed with transferable rewards in mind, as it relies on variations in the environment rather than on a generalizable reward representation.

P. Rolland et al. [25] addresses reward identification from multiple experts acting in environments with discrete state and action spaces. They propose an algorithm to recover rewards by observing how optimal policies vary across different environments, characterized by different transition dynamics or discount factors. However, their method is limited to discrete state spaces and does not extend to continuous states, which significantly constrains its applicability to real-world problems that often involve continuous state spaces. Additionally, their approach is focused on reward identifiability rather than reward transferability.

Viano et al. [31] introduce a robust IRL framework designed to handle transition dynamics mismatch between expert and learner environments. Their method builds on the Maximum Causal Entropy IRL (MCE-IRL) and provides theoretical bounds on performance degradation due to dynamics mismatch. The robust MCE-IRL algorithm leverages adversarial techniques from robust reinforcement learning to mitigate performance loss. While the method is shown to work in both discrete and continuous MDP settings, it still depends on matching the expert’s state occupancy measure across environments, which may not be ideal for scenarios requiring reward transferability.

In contrast, our approach extracts a dynamics-agnostic abstract state using a Variational Autoencoder (VAE), explicitly designed for reward transferability. This abstract state is then used to train a discriminator that distinguishes between expert and generator behaviors, offering a more structured and interpretable learning process. By focusing on key features of the state, independent of the environment’s dynamics, our method enables more effective transfer learning across diverse environments, requiring only one optimal policy per environment.

3 BACKGROUND

Our inverse reinforcement learning method is based on the maximum causal entropy IRL framework as outlined by Ziebart et al. [36]. The entropy-regularized Markov decision process (MDP) is characterized by the tuple $(\mathcal{S}, \mathcal{A}, \mathcal{T}, r, \gamma, \rho_0)$. Here, \mathcal{S} and \mathcal{A} denote the state and action spaces, respectively, while $\gamma \in (0, 1)$ denotes the discount factor. In a standard reinforcement learning context, the dynamics or transition distribution $T(s'|a, s)$, the initial state distribution $\rho_0(s)$, and the reward function $r(s, a)$ are initially unknown, and can only be determined through interaction with the MDP. The optimal policy π under the maximum entropy framework maximizes the objective

$$\pi^* = \arg \max_{\pi} \mathbb{E}_{\tau \sim \pi} \left[\sum_{t=0}^T \gamma^t (r(s_t, a_t) + H(\pi(\cdot|s_t))) \right], \quad (1)$$

where $\tau = (s_0, a_0, \dots, s_T, a_T)$ denotes a sequence of states and actions induced by the policy and transition function.

f -IRL. f -Inverse Reinforcement Learning (f -IRL) [22] is an extension of traditional IRL that integrates f -divergence to improve scalability and robustness. f -IRL (f-IRL) recovers a stationary reward function by matching the expert state marginal distribution, an approach that builds upon and improves the State Marginal Matching (SMM) algorithm. Unlike traditional SMM, which focuses

on implicitly matching state distributions, f -IRL explicitly derives the stationary reward function from the expert state density. This explicit formulation of the reward function provides a more interpretable and direct way to recover the expert policy compared to the original SMM framework. The objective function of f -IRL is defined in the following:

$$\mathcal{L}_f(\theta) = D_f(\rho_E || \rho_\theta) = \int_S f\left(\frac{\rho_E(s)}{\rho_\theta(s)}\right) \rho_\theta(s) ds. \quad (2)$$

Theorem 4.1 (f -divergence analytic gradient) in [22] claims that the analytic gradient of the f -divergence $\mathcal{L}_f(\theta)$ between state marginals of the expert (ρ_E) and the soft-optimal agent w.r.t the reward parameters (θ) is given by:

$$\nabla_\theta \mathcal{L}_f(\theta) = \frac{1}{T} \text{cov}_{\tau \sim \rho_\theta(\tau)} \left(\sum_{t=1}^T h_f\left(\frac{\rho_E(s_t)}{\rho_\theta(s_t)}\right), \sum_{t=0}^T \nabla_\theta r_\theta(s_t) \right), \quad (3)$$

where $h_f(u) \triangleq f(u) - f'(u)u$, $\rho_E(s)$ is the expert state marginal and $\rho_\theta(s)$ is the state marginal of the soft-optimal agent under the reward function r_θ , and the covariance is taken under the agent's trajectory distribution $\rho_\theta(\tau)$. For Reverse Kullback-Leibler (RKL), $f(u) = -\log u$, and thus $h_f(u) = 1 - \log u$.

Variational Autoencoder (VAE). A variational autoencoder [17] is a deep generative model that learns a joint distribution $p(x, z)$ over the observed data x and latent variables z by maximizing the evidence lower bound (ELBO):

$$\mathcal{L}(\theta, \phi; x) = \mathbb{E}_{q_\phi(z|x)} [\log p_\theta(x|z)] - \text{KL}\left(q_\phi(z|x) || p_\theta(z)\right). \quad (4)$$

The ELBO objective consists of a reconstruction term and a KL regularizer that encourages the approximate posterior $q_\phi(z|x)$ (the encoder) to match the prior $p(z)$. The decoder $p_\theta(x|z)$ can then generate new data samples by first sampling $z \sim p(z)$.

Transfer Learning. Transfer learning [35] is a machine learning technique where a model developed in *source domains* is reused as the starting point for a model on *target domains*. This approach leverages the knowledge gained from the source domains, improving learning efficiency and performance in the target domains, particularly when the latter has limited labeled data.

4 LEARNING TRANSFERABLE REWARDS VIA ABSTRACTION

In this section, we describe our method for transferable IRL (T-IRL), which learns an abstract reward function amenable to improved transfer given the expert trajectories in the source environments and can be used forward to learn a well-performing policy in the target environment.

4.1 Learning Abstraction via Multi-Head VAE

To enable reward transfer across different environments, it is important to identify and extract the intrinsic, abstracted information that is invariant and generalizable from the source environment demonstrations. In T-IRL, we use a VAE to uncover the abstraction from the expert and generator trajectory states. Figure 1 visualizes this method. To extract the abstraction from the source environments, we use a *single* environment-agnostic encoder (denoted p_ϕ in Fig. 1) to obtain the abstraction and environment-specific decoders (q_{ψ^i} where i denotes the i -th source task) to reconstruct the state trajectory of each environment. In the training phase, p_ϕ

learns the abstraction from generalizing the states of the source environments. The environment-specific decoders (q_{ψ^i}) learn to reconstruct the states of each environment from the abstraction.

The objective of the VAE is to minimize the loss function:

$$\begin{aligned} \mathcal{L}_{\text{VAE}}(\phi, \psi^1, \dots, \psi^n; \tau) \\ = \sum_{i=1}^n \left(\mathbb{E}_{z \sim p_\phi(z^i|\tau^i)} \left[\log q_{\psi^i}(\tau^i|z) \right] - \lambda_{\text{KLD}} \text{KL}\left(p_\phi(z^i|\tau^i) || p(z^i)\right) \right), \end{aligned} \quad (5)$$

where $\tau = \langle \tau^1, \tau^2, \dots, \tau^i, \dots, \tau^n \rangle$, and τ^i is trajectory from the i -th source environment, $z \sim p_\phi(z^i|\tau^i)$ is the abstracted state sampled from the i -th source environment, ϕ is the parameter of the environment-agnostic encoder p_ϕ , ψ^i is the parameter of the i -th environment-specific decoder q_{ψ^i} , n is the number of source environments, and $p(z^i) = \mathcal{N}(0, 1)$.

4.2 Learning Abstracted State Density Ratio

Instead of having direct access to the experts' policies or state probability densities, in practice, we are provided with expert demonstration trajectories. To estimate the density ratio between the expert and generator state distributions, we employ the Wasserstein-GAN (WGAN) [2] where a discriminator network parameterized by ω , $D_\omega(s)$, is trained to approximate this ratio during each update iteration.

$$D_\omega = \arg \max_{\omega} \mathbb{E}_{s \sim \rho_E(s)} [D_\omega(s)] - \mathbb{E}_{s \sim \rho_\theta(s)} [D_\omega(s)], \quad (6)$$

where $\rho_\theta(s)$ is the state density of generator trajectories and $\rho_E(s)$ is the state density of expert trajectories.

Recall that VAE extracts the abstraction z by optimizing Eq. 5. Substituting state s with abstraction z , where $z \sim q_\phi(z|s)$, we get:

$$D_\omega = \arg \max_{\omega} \mathbb{E}_{z \sim \rho_E(z)} [D_\omega(z)] - \mathbb{E}_{z \sim \rho_\theta(z)} [D_\omega(z)], \quad (7)$$

where $\rho_\theta(z)$ is the abstract state density of generator trajectories and $\rho_E(z)$ is the abstract state density of expert trajectories.

Let $\rho_\theta(z)$ denote the density over the abstracted state representations z induced by the generator's policy and VAE, and $\rho_E(z)$ represent the abstracted state density stemming from the expert demonstration trajectories. It is well known that the optimal discriminator $D_\omega^*(z)$ satisfies

$$D_\omega^*(z) = \frac{\rho_E(z)}{\rho_E(z) + \rho_\theta(z)}.$$

The density ratio between the expert and generator in the abstracted state space can be approximated as $\frac{\rho_E(z)}{\rho_\theta(z)} \approx \frac{D_\omega(z)}{1 - D_\omega(z)}$, where $D_\omega(z)$ is the discriminator parameterized by ω , trained to distinguish between expert and generator states by Eq. 7.

To ensure the stability of training and enforce the 1-Lipschitz constraint required by WGAN, we further impose a gradient penalty on the discriminator (WGAN-GP) [12]. This penalty ensures that the gradients of $D_\omega(z)$ with respect to z remain bounded. The gradient penalty is applied by adding a regularization term to the discriminator's objective function:

$$\mathbb{E}_{z \sim \hat{\rho}(z)} \left[(\|\nabla_z D_\omega(z)\|_2 - 1)^2 \right], \quad (8)$$

where $\hat{\rho}(z)$ is the distribution of points z sampled uniformly along a straight line between expert abstract states drawn from $\rho_E(z)$

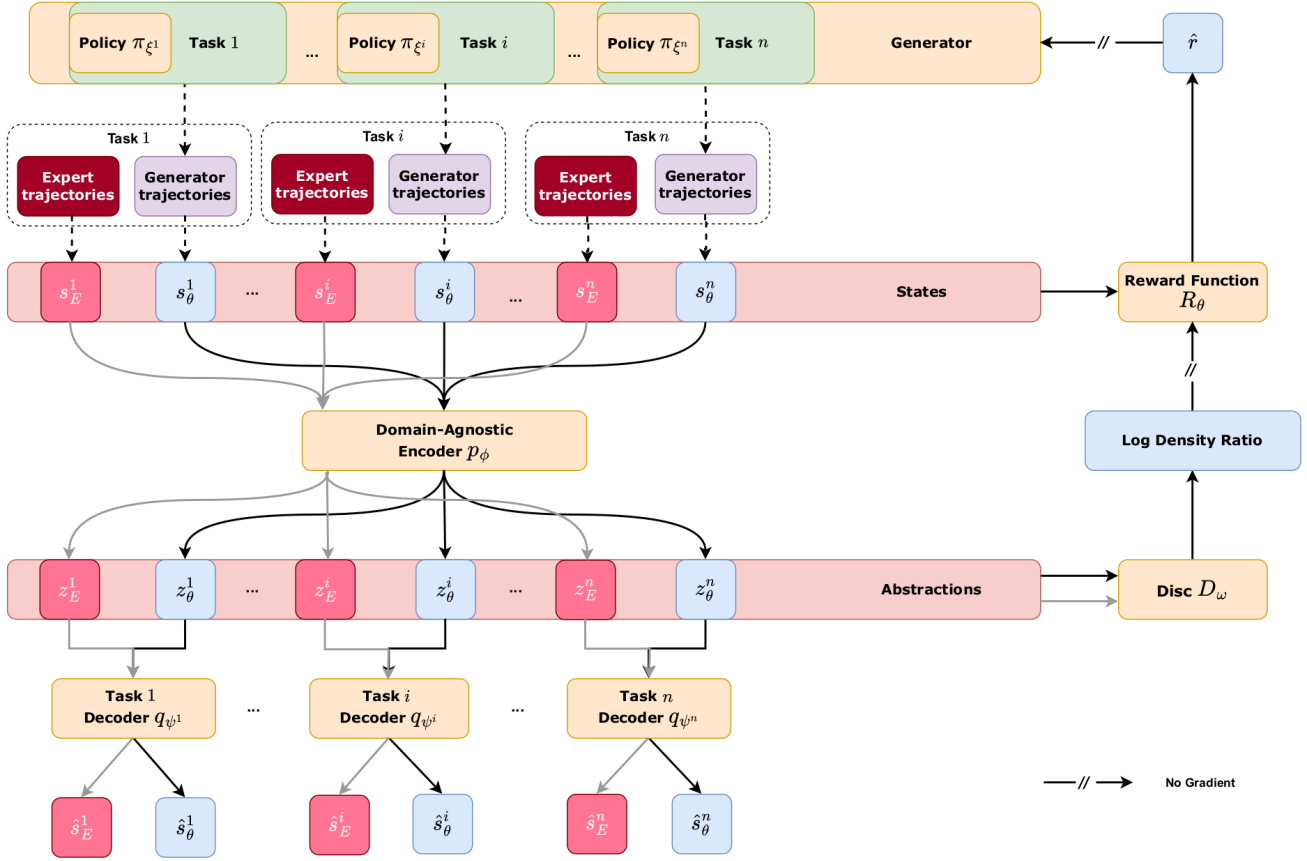


Figure 1: A visualization of the T-IRL method. A multi-head VAE is introduced within the discriminator of a generator-discriminator model. The blue boxes represent the input and output of the neural encoders and decoders which are shown in orange boxes. The green boxes represent the aligned task environments sharing intrinsic preferences. The purple boxes represent the sampled trajectories from the environments. The solid arrow represents the forward updates with backpropagation gradients. The dashed arrow and solid arrow with double slash represent no-gradient forward updates.

and generator abstract states drawn from $\rho_\theta(z)$. This penalty encourages the norm of the gradient of the discriminator with respect to its inputs to be close to 1, satisfying the Lipschitz constraint.

By optimizing the discriminator with this additional gradient penalty, we ensure a more stable training process while preserving the estimation of the density ratio between the expert and generator in the abstract state space.

The objective function for the discriminator is defined as:

$$\begin{aligned} \mathcal{L}_{\text{Disc}}(\omega) = & \mathbb{E}_{z \sim \rho_E(z)} [D_\omega(z)] - \mathbb{E}_{z \sim \rho_\theta(z)} [D_\omega(z)] \\ & + \lambda_{\text{GP}} \mathbb{E}_{z \sim \hat{\rho}(z)} [(\|\nabla_z D_\omega(z)\|_2 - 1)^2], \end{aligned} \quad (9)$$

where $z \sim \rho_E(z)$ is the latent variable z sampled from abstract state density of expert trajectories. $z \sim \rho_\theta(z)$ is the latent variable z sampled from the abstract state density of generator trajectories. D_ω is the discriminator parameterized by ω . $\hat{\rho}(z)$ is the distribution of points z sampled uniformly along a straight line between expert abstract states drawn from $\rho_E(z)$ and generator abstract states

drawn from $\rho_\theta(z)$. λ_{GP} is a regularization coefficient that controls the magnitude of the gradient penalty.

4.3 Robust Reward Learning via Abstracted Density Ratio

Once the abstracted state density ratio is learned, we can recover the reward function based on the abstracted state density ratio in the i -th source environment using Eq. 2 by substituting the states s with the abstracted states z^i in the i -th source environment.

$$\mathcal{L}_f^i(\theta) = D_f(\rho_E || \rho_\theta) = \int f \left(\frac{\rho_E(z^i)}{\rho_\theta(z^i)} \right) \rho_\theta(z^i | s^i) ds^i, \quad (10)$$

where $\frac{\rho_E(z^i)}{\rho_\theta(z^i)}$ is the abstracted density ratio in i -th source environment and n is the number of source environments.

Note that while our approach leverages abstracted state representations extracted by the VAE during the reward learning process, the input to the final learned reward function is the original, unabstracted state. This representation choice ensures that the inversely

learned reward function retains its interpretation as a reward signal, adhering to the standard MDP formulation.

4.4 Analytical Gradient of T-IRL

We derive the analytical form of the gradient for the proposed T-IRL objective Eq. 10. The derivation follows the derivation outlined in the Appendix by Ni et al. [22] except that we use state abstractions z to update the gradient.

From Ni et al. [22], we have the following equations:

$$\begin{aligned} \frac{d\rho_\theta(s)}{d\theta} &= \int \frac{d\rho_\theta(s)}{dr_\theta(s^*)} \frac{dr_\theta(s^*)}{d\theta} ds^* \\ &= \frac{1}{\alpha Z} \int p(\tau) e^{\sum_{t=1}^T r_\theta(s_t)/\alpha} \eta_\tau(s) \sum_{t=1}^T \frac{dr_\theta(s_t)}{d\theta} d\tau \\ &\quad - \frac{T}{\alpha} \rho_\theta(s) \int \rho_\theta(s^*) \frac{dr_\theta(s^*)}{d\theta} ds^*, \end{aligned} \quad (11)$$

where α is the entropy temperature.

The marginal distribution over state abstractions is defined as:

$$\rho_\theta(z|s) = p(z|s) \rho_\theta(s). \quad (12)$$

For simplicity, we will use $\rho_\theta(z)$ to represent $\rho_\theta(z|s)$ in the following derivation.

When applied to the abstraction marginal matching objective between the expert density $\rho_E(z)$ and the generator density $\rho_\theta(z)$ over state space \mathcal{S} in the i -th source environment, the f -divergence objective takes the following form:

$$\begin{aligned} \mathcal{L}_f^i(\theta) &:= D_f(\rho_E \parallel \rho_\theta) \\ &= \int f\left(\frac{\rho_E(z^i)}{\rho_\theta(z^i)}\right) \rho_\theta(z^i) ds \\ &= \int f\left(\frac{\rho_E(z^i)}{\rho_\theta(z^i)}\right) p(z^i|s^i) \rho_\theta(s^i) ds. \end{aligned} \quad (13)$$

The gradient of the f -divergence objective is derived as:

$$\begin{aligned} \nabla_\theta \mathcal{L}_f^i(\theta) &= \int \left(f\left(\frac{\rho_E(z^i)}{\rho_\theta(z^i)}\right) - f'\left(\frac{\rho_E(z^i)}{\rho_\theta(z^i)}\right) \frac{\rho_E(z^i)}{\rho_\theta(z^i)} \right) p(z^i|s^i) \frac{d\rho_\theta(s^i)}{d\theta} ds^i \\ &\triangleq \int h_f\left(\frac{\rho_E(z^i)}{\rho_\theta(z^i)}\right) p(z^i|s^i) \frac{d\rho_\theta(s^i)}{d\theta} ds^i, \end{aligned} \quad (14)$$

where we denote $h_f(u) \triangleq f(u) - f'(u)u$.

Substituting the gradient of state marginal distribution w.r.t θ in Eq.11 (detailed derivation can be found in Ni et al. [22]), we have:

$$\begin{aligned} \nabla_\theta \mathcal{L}_f^i(\theta) &= \frac{1}{\alpha T} \mathbb{E}_{\tau^i \sim \rho_\theta(\tau^i)} \left[\sum_{t=1}^T p(z_t^i|s_t^i) h_f\left(\frac{\rho_E(z_t^i)}{\rho_\theta(z_t^i)}\right) \sum_{t=1}^T \frac{dr_\theta(s_t^i)}{d\theta} \right] \\ &\quad - \frac{T}{\alpha} \mathbb{E}_{s^i \sim \rho_\theta(s^i)} \left[p(z^i|s^i) h_f\left(\frac{\rho_E(z^i)}{\rho_\theta(z^i)}\right) \right] \mathbb{E}_{s^i \sim \rho_\theta^i(s)} \left[\frac{dr_\theta(s^i)}{d\theta} \right]. \end{aligned} \quad (15)$$

To gain further intuition about this equation, we can express all the expectations in terms of trajectories:

$$\begin{aligned} \nabla_\theta \mathcal{L}_f^i(\theta) &= \frac{1}{\alpha T} \text{cov}_{\tau \sim \rho_\theta(\tau^i)} \left(\sum_{t=1}^T p(z_t^i|s_t^i) h_f\left(\frac{\rho_E(z_t^i)}{\rho_\theta(z_t^i)}\right), \sum_{t=1}^T p(z_t^i|s_t^i) \nabla_\theta r_\theta(s_t^i) \right) \\ &= \frac{1}{\alpha T} \text{cov}_{\tau \sim \rho_\theta(\tau^i)} \left(\sum_{t=1}^T h_f\left(\frac{\rho_E(z_t^i)}{\rho_\theta(z_t^i)}\right), \sum_{t=1}^T \nabla_\theta r_\theta(s_t^i) \right). \end{aligned} \quad (16)$$

This gradient formulation efficiently updates the reward function by considering the expert's state densities and the abstracted states over trajectories. It leverages the relationship between the expert and generator densities to guide the reward learning process.

4.5 Transferable Reward Learning

When operating in high-dimensional observation domains, a significant impediment may arise if the state-action visitation distributions induced by the generator's current policy substantially diverge from the expert demonstration trajectories. Under such conditions of distributional mismatch, we empirically find that the gradient signal derived from our proposed objective function, Eq. 16, provides limited supervisory information to guide the policy optimization process. We follow the technique introduced by Finn et al. [6], mixing the data samples from expert trajectories with the generator trajectories data. The revised objective function is then given by the following:

$$\mathcal{L}_f^i(\theta) = \frac{1}{\alpha T} \sum_{i=1}^n \left(\text{cov}_{\tau \sim \hat{\rho}(\tau^i)} \left(\sum_{t=1}^T h_f\left(\frac{\rho_E(z_t^i)}{\rho_\theta(z_t^i)}\right), \sum_{t=0}^T r_\theta(s_t^i) \right) \right), \quad (17)$$

where $\frac{\rho_E(z_t^i)}{\rho_\theta(z_t^i)}$ is the abstracted density ratio in the i -th source environment, $\hat{\rho}(\tau^i) = \frac{1}{2}(\rho_\theta(\tau^i) + \rho_E(\tau_E^i))$, n is the number of source environments.

The overall objective function for T-IRL is defined as:

$$\begin{aligned} \min \mathcal{L}(\theta, \omega, \phi, \psi^1, \dots, \psi^n) \\ = \mathcal{L}_f^i(\theta) - \mathcal{L}_{\text{VAE}}(\phi, \psi^1, \dots, \psi^n) - \mathcal{L}_{\text{Disc}}(\omega). \end{aligned} \quad (18)$$

As established by Fu et al. [7], reward functions that are disentangled from the dynamics of the environment are desirable for transferability, as they can generalize across different environments. The AIRL paper [7] demonstrates that if a reward function is agnostic to the dynamics, it must be a state-only reward function. However, the reverse is not necessarily true—a state-only reward function does not guarantee dynamic independence.

THEOREM 1. *If a reward function $r'(s, a, s')$ is disentangled for all dynamics functions, then it must be state-only. i.e. If for all dynamics T ,*

$$Q_{r', T}^*(s, a) = Q_{r', T}^*(s, a) + f(s) \quad \forall s, a.$$

Then r' is only a function of state.

In our approach, the abstracted state representation is designed to capture sufficient information to remain invariant to the dynamics. By training the discriminator and the VAE across multiple source environments, we aim to capture a representation that generalizes well and is robust to changes in dynamics. This facilitates the shaping of the reward function towards dynamic-agnostic behavior, as the updated discriminator distinguishes expert and generator

behaviors across different source environments. As a result, the reward function learned by T-IRL can be adapted to be agnostic to dynamics, enabling high transferability across diverse environments.

Extracting common and invariant knowledge across different tasks also aids learning a transferable reward function. T-IRL fulfills this desired criterion through the multi-head VAE to derive abstracted representations from the states. While the learned rewards may not be a direct function of the abstraction, the learning of the rewards involves the discriminator which utilizes the abstraction as its input. More specifically, the reward learning procedure relies on a discriminator network that takes the abstracted states as input. This discriminator is optimized to distinguish between the distributions over the abstracted representations induced by the expert demonstrations and the generator’s policy. The reward function is then shaped by the density ratio over the abstracted state space provided by this discriminator.

Algorithm 1 T-IRL: *Training Phase*

Require: Expert trajectories $\tau_E^1, \dots, \tau_E^n$, Number of source environments: n

- 1: Initialize generator policy $\pi_{\xi_1}, \dots, \pi_{\xi_n}$, Trajectory buffer B , Discriminator D_ω , Reward function R_θ , encoder of VAE q_ϕ , and decoders of VAE $p_{\psi^1}, \dots, p_{\psi^n}$
- 2: Add expert trajectories $\tau_E^1, \dots, \tau_E^n$ into trajectory buffer B
- 3: **while** not converged **do**
- 4: **for** env i in $1, \dots, n$ **do**
- 5: Collect trajectories $\tau^i = (s_0, a_0, \dots, s_T, a_T)$ by executing π_{ξ_i}
- 6: Add trajectories τ^i into trajectory buffer B
- 7: **end for**
- 8: Sample trajectories $\bar{\tau}$ from Buffer B
- 9: Update encoder of VAE q_ϕ , decoders of VAE $p_{\psi^1}, \dots, p_{\psi^n}$ using sampled trajectories $\bar{\tau}$ by Eq. (5)
- 10: Update Discriminator D_ω using trajectories $\bar{\tau}$ by Eq. (9)
- 11: Update Reward function R_θ using trajectories $\bar{\tau}$ by Eq. (16)
- 12: Update generator policy $\pi_{\xi_1}, \dots, \pi_{\xi_n}$ using Reward function R_θ
- 13: **end while**

Algorithm 2 T-IRL: *Transfer Testing Phase*

Require: Learned abstract reward function R_θ , Target Environment E

- 1: Initialize policy π_ξ
- 2: **while** Policy π_ξ not converged **do**
- 3: Update policy π_ξ using the learned transferable reward function R_θ in target environment E
- 4: **end while**

5 EXPERIMENTS

To further empirically validate and evaluate the efficiency of our method, T-IRL, we conduct experiments across multiple Mujoco [30] benchmark domains and AssistiveGym domains [5]. In our experiments, we measure the average true reward accrued over 25 episodes by T-IRL and compare it against several state-of-the-art methods, including AIRL [7], f -IRL [22], and I2L [8].

Although AIRL and f -IRL were not specifically designed to learn transferable reward functions, their respective papers suggest that these algorithms can generalize rewards across environments with

dynamic shifts. However, their focus on single-environment contexts limits their robustness in dealing with varying dynamics, which we will examine in the following experiments.

In contrast, I2L is tailored to handle dynamic shifts and is more suitable for generalization across different environments. However, the absence of an abstraction mechanism in I2L leads to training instability and reduced interpretability. By integrating an abstract state representation learned through VAE, T-IRL achieves more stable and interpretable training while maintaining dynamics-agnostic reward generalization. The following experiments empirically validate our approach’s superiority.

Through these experiments, we examine T-IRL’s capacity to generalize and learn a transferable reward function as compared to the baselines.

We employ multilayer perceptron (MLP) architectures for both the reward function and VAE, using Tanh as the activation function. For comparison, the baseline methods (AIRL, f -IRL) parameterize their reward functions and discriminators as state-only. In handling multiple source environments, these baselines simply feed states directly from the source environments into the discriminator without any additional modification or adaptation. We adopt the Soft Actor-Critic (SAC) [13] as the base maxEnt RL framework. We choose reverse KL divergence (RKL) as the objective function in f -IRL because RKL has been proven to be more robust and faster to converge in the IRL setting [11, 22]. Comprehensive details regarding the training and hyperparameter are provided in the Appendix.

5.1 Transfer Learning Training and Evaluation Pipeline

Training on Source Environments We begin by training both the baseline methods (AIRL, f -IRL, I2L) and our proposed method (T-IRL) on two distinct source environments, each characterized by different dynamics to promote robustness and generalization. Each algorithm is trained until convergence, defined by the cumulative reward of both the learned reward function and the ground truth reward function reaching a steady state.

Transfer to Unseen Target Environment Once the training in the source environments is complete and the reward functions have converged, we evaluate the transferability of the learned reward function by applying it to an unseen target environment. In this transfer learning phase, we use the learned reward function to train a new policy from scratch in the target environment.

Evaluation The performance of the transferred reward function is evaluated by measuring the cumulative true reward achieved by the new policy in the target environment. This allows us to compare the transferability and robustness of the reward functions learned by T-IRL and the baseline methods.

5.2 Transfer Learning for Inverse Reinforcement Learning

We empirically evaluate the effectiveness of the proposed T-IRL methodology in enabling transfer learning across diverse environments with respect to reward function generalization.

5.2.1 Experimental Result. We use HalfCheetah and Ant as the testbed. There are two source and one target environments for

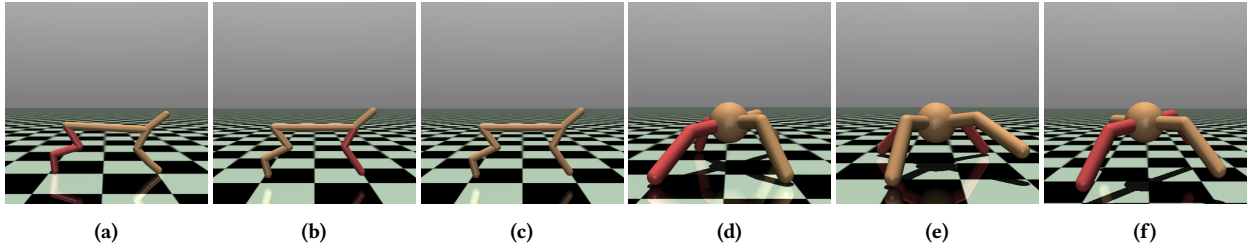


Figure 2: Source and Target Environments in Mujoco domains. The red legs represents the disabled legs of the robots. Figure 2a and 2b are the source environments for HalfCheetah. Figure 2c is the target environment for HalfCheetah. Figure 2d and 2e are the source environments for Ant. Figure 2f is the target environment for Ant.

HalfCheetah. There are two source and one target environments for Ant as well. Figure 2 shows the details about the source and target environments. The dynamics of the source and target environments are different. The details of the environments and training curves are listed in the Appendix.

The empirical result is reported by Table 1 and Table 2. The proposed T-IRL method achieves the highest average return across both source and target environments for HalfCheetah and Ant. The performance of T-IRL in the target environments is competitive with or even exceeds its performance in the source environments, demonstrating effective transfer learning capabilities. Other IRL or IL methods like AIRL, and f -IRL exhibit varying degrees of performance degradation when transferring from source to target environments, indicating limitations in learning transferable reward functions.

Table 1: Actual cumulative reward with standard deviation in the HalfCheetah environment. The bold method statistically outperforms other methods ($p < 0.01$).

	HalfCheetah		
	Source Env 1	Source Env 2	Target Env
BC	251.38 ± 153.73	204.79 ± 131.10	166.73 ± 173.76
AIRL	2573.91 ± 82.45	1576.82 ± 529.99	2683.81 ± 163.82
f -IRL	3252.72 ± 67.90	3523.01 ± 91.06	3582.10 ± 94.32
I2L	4396.43 ± 45.37	4518.66 ± 52.19	4512.71 ± 66.37
T-IRL	4404.07 ± 57.63	4359.35 ± 99.24	4745.59 ± 48.56
Expert	5052.25 ± 25.39	5499.07 ± 156.06	7589.52 ± 123.55

5.2.2 *Visualization of Abstractions.* Figure 3 depicts the visualization of states and abstractions from HalfCheetah source environments. Figure 3a illustrates the *sparse* distribution of states across two source domains, contrasting the expert and generator trajectories. The state distributions exhibit noticeable differences between the environments, reflecting environment-specific characteristics. On the other hand, Figure 3b depicts the *dense* distribution of the learned abstractions from the same two source environments. Notably, the abstraction distributions are more focused on distinguishing between expert and generator trajectories, while being largely invariant to the specific source domain. This concentration on discriminating expert vs. generator behavior, while disregarding

environment-specific factors in the abstraction space, is a desirable property for effective transfer learning. The key to enabling generalization to target environments lies in learning a unified distribution over the abstractions that captures the shared structure present across all individual source domains.

Table 2: Actual cumulative reward with standard deviation in the Ant environment. The bold method statistically outperforms other methods ($p < 0.01$).

	Ant		
	Source Env 1	Source Env 2	Target Env
BC	42.68 ± 298.53	71.41 ± 194.87	57.10 ± 232.84
AIRL	1918.28 ± 76.32	1415.76 ± 83.78	947.00 ± 37.84
f -IRL	2456.17 ± 85.01	1146.39 ± 95.82	1598.24 ± 44.90
I2L	2831.28 ± 36.36	2786.90 ± 79.39	2585.32 ± 84.48
T-IRL	2714.18 ± 35.86	2936.52 ± 95.46	2917.92 ± 79.29
Expert	3312.12 ± 304.32	3303.99 ± 341.03	5554.23 ± 15.98

5.3 Transfer Learning for Robots in Simulation

In this subsection, we empirically evaluate the proposed T-IRL methodology within the AssistiveGym environment, a simulation platform designed for robotic assistive tasks. One key difference between the MuJoCo environments and AssistiveGym is the nature of the reward functions. In MuJoCo environments, there is no external reward function aside from the learned reward function. However, AssistiveGym is a goal-based environment with explicit terminal states and corresponding rewards.

In AssistiveGym, other than the rewards assigned to the terminal states, there is no reward available except for the learned reward function. For instance, in the FeedingSawyer environment, if the robot spills food from the spoon, it enters a terminal state with a reward of -1. Conversely, if the robot successfully feeds the human, the agent receives a +10 reward upon reaching the terminal state. Throughout the rest of the task, the agent relies entirely on the learned reward function to guide its behavior. This reliance on learned rewards, combined with explicit terminal rewards, presents a unique challenge compared to the MuJoCo environments, where no predefined terminal or goal-based rewards exist.

For the source environments, we selected FeedingSawyer, Fig 4, a simulation environment in which the robot (Sawyer) is tasked

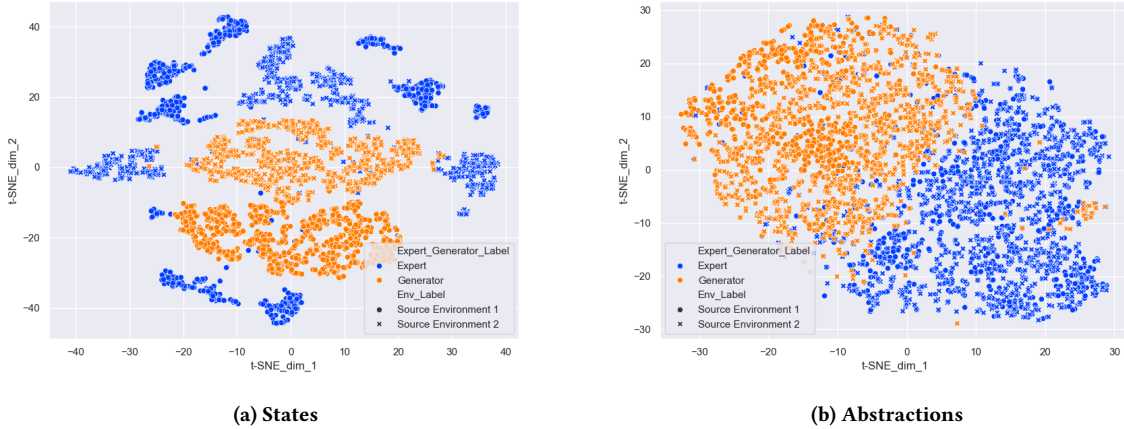


Figure 3: Visualization of distributions of states and abstractions for HalfCheetah source environments using t-SNE.

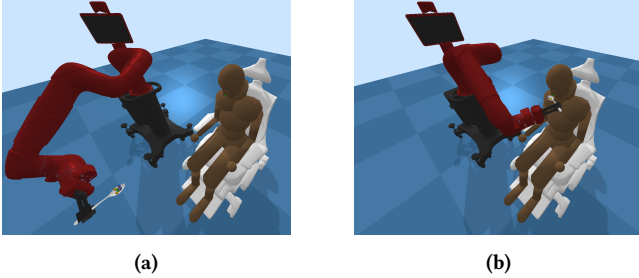


Figure 4: Initial and goal positions in the FeedingSawyer environment from AssistiveGym. (a) The initial configuration. (b) The goal configuration, where the spoon is positioned close enough to the human’s mouth for feeding assistance.



Figure 5: Initial and goal positions in the ScratchItchSawyer environment from AssistiveGym. (a) The initial configuration. (b) The goal configuration, where the robot arm is positioned to scratch the target area, close enough to alleviate the itch.

with feeding a disabled human. In this setup, the robot must learn to maneuver a spoon filled with food towards the human’s mouth. To introduce variability and test robustness, we use different types of disabled human models in these source environments. The robot’s challenge is to adapt to different human conditions while executing the feeding task effectively. In contrast, for the target environment,

we selected ScratchItchSawyer, Fig 5. In this simulation environment, the same robot (Sawyer) must learn to move its end effector to a specific itch area on the human’s forearm. Although this task differs from feeding in terms of its specific goal, the essence of both tasks remains the same: the robot is required to move its end effector precisely to a designated target area.

Table 3 presents the performance of various IRL methods in the AssistiveGym environment, both in source and target tasks. The results show that I2L performs well in the two source environments, achieving reward values close to the expert, as it effectively leverages variations in dynamics or discount factors to identify the true reward function. However, I2L’s reward function is highly specific to the source environments, leading to a significant drop in performance when transferred to the target environment indicating poor transferability.

In contrast, T-IRL demonstrates consistent performance across both source and target environments, showcasing its superior transferability. AIRL and f -IRL exhibit consistently negative rewards across all tasks, highlighting their difficulty in generalizing to new environments. Overall, T-IRL shows better generalization and robustness, successfully transferring the learned reward function across different tasks, while the baseline methods.

Table 3: Actual cumulative reward with standard deviation in the AssistiveGym environments. The bold method statistically outperforms other methods.

	AssistiveGym		
	Feeding (Source Env 1)	Feeding (Source Env 2)	Scratch Itch (Target Env)
BC	-74.89 ± 42.61	-80.57 ± 53.67	-92.11 ± 52.73
AIRL	-13.22 ± 13.56	-18.30 ± 19.26	-22.36 ± 15.31
f -IRL	-10.63 ± 16.79	-15.34 ± 22.78	-21.35 ± 14.89
I2L	9.32 ± 11.84	9.11 ± 11.36	-10.07 ± 8.02
T-IRL	8.32 ± 7.91	9.56 ± 10.52	-3.82 ± 3.33
Expert	11.29 ± 5.39	12.77 ± 4.28	-1.18 ± 5.71

Table 4 presents the Pearson correlation coefficient between the learned reward and the true reward. The correlation coefficient of

Table 4: Pearson correlation between the true reward and the learned reward in the ScratchItchSawyer environment.

Pearson Correlation	p-value
0.8553	9.66×10^{-156}

0.8553 indicates a strong positive linear relationship, meaning that the learned reward aligns closely with the true reward. This suggests that the learning process has been effective in approximating the true reward function.

5.4 Ablation Study

Table 5: Actual cumulative reward with standard deviation in the HalfCheetah environment. The bold method statistically outperforms other methods ($p < 0.01$).

	HalfCheetah		
	Source Env 1	Source Env 2	Target Env
$\lambda_{GP} = 1$	4646.12 \pm 40.61	4602.13 \pm 24.11	3228.27 \pm 185.48
$\lambda_{GP} = 5$	4498.74 \pm 59.51	4313.89 \pm 54.39	3989.06 \pm 61.59
$\lambda_{GP} = 10$	4404.07 \pm 57.63	4359.35 \pm 99.24	4745.59 \pm 48.56
$\lambda_{GP} = 100$	172.69 \pm 191.88	155.66 \pm 159.59	150.41 \pm 102.58
Expert	5052.25 \pm 25.39	5499.07 \pm 156.06	7589.52 \pm 123.55

5.4.1 Ablation Study on λ_{GP} . The results indicate that $\lambda_{GP} = 10$ achieves the best balance between source and target environments. Smaller values like $\lambda_{GP} = 1$ perform well in the source environments but show weaker transferability to the target environment. Larger values like $\lambda_{GP} = 100$ result in a significant drop in performance across all environments, likely due to over-smoothing of the discriminator. This suggests that $\lambda_{GP} = 10$ provides an optimal trade-off, ensuring stable training and effective reward transfer.

Table 6: Actual cumulative reward with standard deviation in the HalfCheetah environment. The bold method statistically outperforms other methods ($p < 0.01$).

	HalfCheetah		
	Source Env 1	Source Env 2	Target Env
$\lambda_{KLD} = 0.05$	4323.23 \pm 29.58	4471.05 \pm 56.21	4541.09 \pm 96.30
$\lambda_{KLD} = 0.1$	4404.07 \pm 57.63	4359.35 \pm 99.24	4745.59 \pm 48.56
$\lambda_{KLD} = 0.25$	4430.26 \pm 62.69	4234.33 \pm 84.04	4548.23 \pm 44.49
$\lambda_{KLD} = 0.5$	3806.92 \pm 85.43	3888.79 \pm 52.48	4088.95 \pm 83.82
Expert	5052.25 \pm 25.39	5499.07 \pm 156.06	7589.52 \pm 123.55

5.4.2 Ablation Study on λ_{KLD} . The results show that $\lambda_{KLD} = 0.1$ achieves the best overall performance. This indicates that moderate regularization balances reconstruction and generalization in the VAE, leading to better transferability. For $\lambda_{KLD} = 0.05$, slightly weaker target performance suggests insufficient regularization, allowing the VAE to overfit to source environments. Increasing λ_{KLD}

to 0.25 maintains competitive performance in the target environment but results in a noticeable drop in the source environments. At $\lambda_{KLD} = 0.5$, the regularization becomes too strong, leading to significant performance degradation across both source and target environments. This highlights the importance of tuning λ_{KLD} to achieve optimal abstraction in the VAE for effective reward transfer.

Table 7: Actual cumulative reward with standard deviation in the HalfCheetah environment. The bold method statistically outperforms other methods ($p < 0.01$).

	HalfCheetah		
	Source Env 1	Source Env 2	Target Env
RKL	4404.07 \pm 57.63	4359.35 \pm 99.24	4745.59 \pm 48.56
FKL	180.57 \pm 11.07	127.58 \pm 31.89	159.67 \pm 74.45
JS	3889.58 \pm 43.66	3576.25 \pm 79.77	3763.93 \pm 65.94
Expert	5052.25 \pm 25.39	5499.07 \pm 156.06	7589.52 \pm 123.55

5.4.3 Ablation Study on f -divergence. The results highlight the impact of different divergence measures on performance. The Reverse KL (RKL) divergence achieves the best overall performance across all environments. This suggests that RKL effectively aligns the learned reward function with the expert demonstrations, enabling superior transferability. The Forward KL (FKL) divergence performs poorly in all environments, with rewards significantly lower than other methods. This can be attributed to FKL’s tendency to overly penalize areas where the learned distribution deviates from the expert’s, leading to unstable training and limited generalization. The Jensen-Shannon (JS) divergence achieves intermediate performance. While better than FKL, JS fails to match the performance of RKL, possibly due to its symmetric nature, which may not prioritize aligning the generator distribution with the expert as strongly as RKL.

6 CONCLUSION AND LIMITATION

In conclusion, the proposed T-IRL framework represents a significant advancement in inverse reinforcement learning by introducing a principled approach to learn transferable reward functions from expert demonstrations across multiple source environments. The key innovation lies in the ability to extract invariant abstractions that encode the intrinsic structure of expert and generator trajectories while remaining agnostic to environment-specific factors.

While our experiments address environments with varying dynamics and reward functions, the state spaces across the transfer tasks were consistent. Extending T-IRL to scenarios with heterogeneous state spaces will require additional efforts for representation alignment, which are beyond the scope of this paper. Future work will focus on incorporating state alignment techniques into the T-IRL pipeline, enabling more generalizable transfer across diverse environments. The reward function also struggles to handle entirely unseen movements that are critical to the target task.

REFERENCES

- [1] Cameron Allen, Neev Parikh, Omer Gottesman, and George Konidaris. 2021. Learning markov state abstractions for deep reinforcement learning. *Advances in Neural Information Processing Systems* 34 (2021), 8229–8241.
- [2] Martin Arjovsky, Soumith Chintala, and Léon Bottou. 2017. Wasserstein Generative Adversarial Networks. In *Proceedings of the 34th International Conference on Machine Learning (Proceedings of Machine Learning Research, Vol. 70)*. Doina Precup and Yee Whye Teh (Eds.). PMLR, 214–223. <https://proceedings.mlr.press/v70/arjovsky17a.html>
- [3] Saurabh Arora and Prashant Doshi. 2021. A survey of inverse reinforcement learning: Challenges, methods and progress. *Artificial Intelligence* 297 (2021), 103500. <https://doi.org/10.1016/j.artint.2021.103500>
- [4] Haoyang Cao, Samuel N. Cohen, and Lukasz Szpruch. 2024. Identifiability in inverse reinforcement learning. In *Proceedings of the 35th International Conference on Neural Information Processing Systems (NIPS '21)*. Curran Associates Inc., Red Hook, NY, USA, Article 946, 12 pages.
- [5] Zackory Erickson, Vamsee Gangaram, Ariel Kapusta, C. Karen Liu, and Charles C. Kemp. 2019. Assistive Gym: A Physics Simulation Framework for Assistive Robotics. *CoRR* abs/1910.04700 (2019). [arXiv:1910.04700](http://arxiv.org/abs/1910.04700) <http://arxiv.org/abs/1910.04700>
- [6] Chelsea Finn, Sergey Levine, and Pieter Abbeel. 2016. Guided cost learning: Deep inverse optimal control via policy optimization. In *International conference on machine learning*. PMLR, 49–58.
- [7] Justin Fu, Katie Luo, and Sergey Levine. 2018. Learning Robust Rewards with Adversarial Inverse Reinforcement Learning. In *International Conference on Learning Representations*.
- [8] Tanmay Gangwani and Jian Peng. 2020. State-only Imitation with Transition Dynamics Mismatch. In *8th International Conference on Learning Representations, ICLR 2020, Addis Ababa, Ethiopia, April 26-30, 2020*. OpenReview.net. <https://openreview.net/forum?id=HjgLLyrYwB>
- [9] Divyansh Garg, Shuvam Chakraborty, Chris Cundy, Jiaming Song, and Stefano Ermon. 2021. Iq-learn: Inverse soft-q learning for imitation. *Advances in Neural Information Processing Systems* 34 (2021), 4028–4039.
- [10] Carl Friedrich Gauss and Charles Henry Davis. 1857. Theory of the motion of the heavenly bodies moving about the sun in conic sections. *Gauss's Theoria Motus* 76, 1 (1857), 5–23.
- [11] Seyed Kamyar Seyed Ghasemipour, Richard Zemel, and Shixiang Gu. 2020. A divergence minimization perspective on imitation learning methods. In *Conference on robot learning*. PMLR, 1259–1277.
- [12] Ishaan Gulrajani, Faruk Ahmed, Martin Arjovsky, Vincent Dumoulin, and Aaron Courville. 2017. Improved training of wasserstein GANs. In *Proceedings of the 31st International Conference on Neural Information Processing Systems (Long Beach, California, USA) (NIPS'17)*. Curran Associates Inc., Red Hook, NY, USA, 5769–5779.
- [13] Tuomas Haaroja, Aurick Zhou, Pieter Abbeel, and Sergey Levine. 2018. Soft actor-critic: Off-policy maximum entropy deep reinforcement learning with a stochastic actor. In *International conference on machine learning*. PMLR, 1861–1870.
- [14] Michael Herman, Tobias Gindele, Jörg Wagner, Felix Schmitt, and Wolfram Burgard. 2016. Inverse reinforcement learning with simultaneous estimation of rewards and dynamics. In *Artificial intelligence and statistics*. PMLR, 102–110.
- [15] Jonathan Ho and Stefano Ermon. 2016. Generative adversarial imitation learning. *Advances in neural information processing systems* 29 (2016).
- [16] Yachen Kang, Jinxin Liu, and Donglin Wang. 2024. Off-Dynamics Inverse Reinforcement Learning. *IEEE Access* (2024).
- [17] Diederik P Kingma and Max Welling. 2013. Auto-encoding variational bayes. *arXiv preprint arXiv:1312.6114* (2013).
- [18] Joseph-Louis Lagrange. 1788. *Mécanique Analytique*. Desaint, Paris.
- [19] Lisa Lee, Benjamin Eysenbach, Emilio Parisotto, Eric Xing, Sergey Levine, and Ruslan Salakhutdinov. 2019. Efficient exploration via state marginal matching. *arXiv preprint arXiv:1906.05274* (2019).
- [20] Jorge Mendez, Shashank Shivkumar, and Eric Eaton. 2018. Lifelong inverse reinforcement learning. *Advances in neural information processing systems* 31 (2018).
- [21] Andrew Y Ng, Stuart Russell, et al. 2000. Algorithms for inverse reinforcement learning. In *icml*, Vol. 1. 2.
- [22] Tianwei Ni, Harshit Sikchi, Yufei Wang, Tejus Gupta, Lisa Lee, and Ben Eysenbach. 2021. f-irl: Inverse reinforcement learning via state marginal matching. In *Conference on Robot Learning*. PMLR, 529–551.
- [23] Deepak Ramachandran and Eyal Amir. 2007. Bayesian Inverse Reinforcement Learning. In *IJCAI*, Vol. 7. 2586–2591.
- [24] Paul Rolland, Luca Viano, Norman Schürhoff, Boris Nikolov, and Volkan Cevher. 2022. Identifiability and generalizability from multiple experts in inverse reinforcement learning. *Advances in Neural Information Processing Systems* 35 (2022), 550–564.
- [25] Paul Rolland, Luca Viano, Norman Schürhoff, Boris Nikolov, and Volkan Cevher. 2024. Identifiability and generalizability from multiple experts in inverse reinforcement learning. In *Proceedings of the 36th International Conference on Neural Information Processing Systems (New Orleans, LA, USA) (NIPS '22)*. Curran Associates Inc., Red Hook, NY, USA, Article 40, 15 pages.
- [26] Andreas Schlaginhausen and Maryam Kamgarpour. 2024. Towards the Transferability of Rewards Recovered via Regularized Inverse Reinforcement Learning. *arXiv preprint arXiv:2406.01793* (2024).
- [27] John Schulman, Philipp Moritz, Sergey Levine, Michael Jordan, and Pieter Abbeel. 2018. High-Dimensional Continuous Control Using Generalized Advantage Estimation. [arXiv:1506.02438](https://arxiv.org/abs/1506.02438) [cs.LG]
- [28] Prasanth Sengodu Suresh, Yikang Gui, and Prashant Doshi. 2023. Dec-AIRL: Decentralized Adversarial IRL for Human-Robot Teaming. In *Proceedings of the 2023 International Conference on Autonomous Agents and Multiagent Systems*. 1116–1124.
- [29] Ajay Kumar Tanwani and Aude Billard. 2013. Transfer in inverse reinforcement learning for multiple strategies. In *2013 IEEE/RSJ International Conference on Intelligent Robots and Systems*. 3244–3250.
- [30] Emanuel Todorov, Tom Erez, and Yuval Tassa. 2012. MuJoCo: A physics engine for model-based control. In *2012 IEEE/RSJ International Conference on Intelligent Robots and Systems*. 5026–5033. <https://doi.org/10.1109/IROS.2012.6386109>
- [31] Luca Viano, Yu-Ting Huang, Parameswaran Kamalaruban, Adrian Weller, and Volkan Cevher. 2024. Robust inverse reinforcement learning under transition dynamics mismatch. In *Proceedings of the 35th International Conference on Neural Information Processing Systems (NIPS '21)*. Curran Associates Inc., Red Hook, NY, USA, Article 1984, 15 pages.
- [32] Se-Wook Yoo and Seung-Woo Seo. 2022. Learning multi-task transferable rewards via variational inverse reinforcement learning. In *2022 International Conference on Robotics and Automation (ICRA)*. IEEE, 434–440.
- [33] Lantao Yu, Tianhe Yu, Chelsea Finn, and Stefano Ermon. 2019. Meta-inverse reinforcement learning with probabilistic context variables. *Advances in neural information processing systems* 32 (2019).
- [34] Kevin Zakka, Andy Zeng, Pete Florence, Jonathan Tompson, Jeannette Bohg, and Debidatta Dwibedi. 2022. Xirl: Cross-embodiment inverse reinforcement learning. In *Conference on Robot Learning*. PMLR, 537–546.
- [35] Fuzhen Zhuang, Zhiyuan Qi, Keyu Duan, Dongbo Xi, Yongchun Zhu, Hengshu Zhu, Hui Xiong, and Qing He. 2020. A Comprehensive Survey on Transfer Learning. [arXiv:1911.02685](https://arxiv.org/abs/1911.02685) [cs.LG]
- [36] Brian D. Ziebart, J. Andrew Bagnell, and Anind K. Dey. 2010. Modeling interaction via the principle of maximum causal entropy. In *Proceedings of the 27th International Conference on Machine Learning (Haifa, Israel) (ICML '10)*. Omnipress, Madison, WI, USA, 1255–1262.